Testing the Gamma-Ray Burst Energy Relationships

David L. Band[1,2] and Robert D. Preece[3]

dband@lheapop.gsfc.nasa.gov, rob.preece@msfc.nasa.gov

ABSTRACT

Building on Nakar & Piran's analysis of the Amati relation relating gamma-ray burst peak energies E_p and isotropic energies $E_{\rm iso}$, we test the consistency of a large sample of BATSE bursts with the Amati and Ghirlanda (which relates peak energies and actual gamma-ray energies E_γ) relations. Each of these relations can be expressed as a ratio of the different energies that is a function of redshift (for both the Amati and Ghirlanda relations) and beaming fraction f_B (for the Ghirlanda relation). The most rigorous test, which allows bursts to be at any redshift, corroborates Nakar & Piran's result—88% of the BATSE bursts are inconsistent with the Amati relation—while only 1.6% of the bursts are inconsistent with the Ghirlanda relation if $f_B = 1$. Modelling the redshift distribution results in an energy ratio distribution for the Amati relation that is shifted by an order of magnitude relative to the observed distributions; any sub-population satisfying the Amati relation can comprise at most $\sim 18\%$ of our burst sample. A similar analysis of the Ghirlanda relation depends sensitively on the beaming fraction distribution for small values of f_B; for reasonable estimates of this distribution about a third of the burst sample is inconsistent with the Ghirlanda relation. Our results indicate that these relations are an artifact of the selection effects of the burst sample in which they were found; these selection effects may favor sub-populations for which these relations are valid.

Subject headings: gamma-rays: bursts

---

[1]GLAST SSC, Code 661, NASA/Goddard Space Flight Center, Greenbelt, MD 20771

[2]Joint Center for Astrophysics, Physics Department, University of Maryland Baltimore County, 1000 Hilltop Circle, Baltimore, MD 21250

[3]Department of Physics, University of Alabama in Huntsville, Huntsville, AL 35899

1. Introduction

Recently correlations between various energies characterizing gamma-ray bursts have been reported (Amati et al. 2002; Ghirlanda, Ghisellini & Lazzati 2004). If true, these correlations have significant implications for burst physics, and could supplement incomplete observations in compiling burst databases. Building on Nakar & Piran (2004), we test these relations for consistency with a subset of the bursts observed by the Burst and Transient Source Experiment (BATSE) that flew on the *Compton Gamma-Ray Observatory (CGRO)*. Note that consistency would not prove the validity of these relations.

Amati et al. (2002) found that the peak energy E_p, the energy of the peak of $E^2N(E) \propto \nu f_\nu$ for the entire burst, and the apparent isotropic energy $E_{\rm iso}$, the total burst energy if the observed flux were radiated in all directions, are related: $E_p \propto E_{\rm iso}^{1/2}$. This is the Amati relation. Subsequently Ghirlanda et al. (2004) found that E_p and the actual emitted energy E_γ are even more tightly correlated: $E_p \propto E_\gamma^{0.7}$. This is the Ghirlanda relation. In these relations E_p is in the burst frame, and is found by fitting the spectrum of the 'fluence spectrum,' the spectrum formed from summing all the burst emission. $E_{\rm iso}$ is calculated from the observed bolometric energy fluence using the burst redshift, while E_γ is determined from $E_{\rm iso}$ with corrections for the beaming of the gamma-ray emission derived from analyzing afterglows. These relations were discovered and calibrated using the small number of bursts for which afterglows and redshifts have been determined. The calibrating burst database is small and heterogeneous enough that the fitted parameters of these relations are sensitive to the editing of the burst database; for example, see Friedman & Bloom (2004). In addition, the sample is subject to selection effects resulting from localizing the burst in different wavebands, tracking the afterglow, and determining the redshift of the afterglow or the host galaxy.

Nakar & Piran (2004) pointed out that while larger burst databases lack the redshifts necessary to calibrate the Amati relation, these databases can test the validity of this relation because the ratio $E_p^2/E_{\rm iso}$ cannot exceed a maximum value for all redshifts. They found that a large fraction of the bursts in the databases they considered cannot satisfy the Amati relation.

We build on the work of Nakar & Piran (2004) using a database of 760 BATSE bursts with observed $E_{p,obs}$ and fluences, and test both the Amati and Ghirlanda relations. To calculate E_γ for the Ghirlanda relation we need the beaming fraction f_B, for which an afterglow must be detected and monitored. The most rigorous test assumes $f_B = 1$, in which case the Ghirlanda relation becomes the Amati relation—$E_{\rm iso} = E_\gamma$ when $f_B = 1$—albeit with a different exponent for E_p. We find that indeed a large fraction of the bursts in our sample are inconsistent with the Amati relation, as Nakar & Piran found, but only a

small fraction are inconsistent with the Ghirlanda relation under the extreme condition that $f_B = 1$.

These rigorous tests of these two relations put bursts at the redshift that maximizes the $E_p^2/E_{\rm iso}$ and $E_p^{0.7}/E_\gamma$ ratios, and for the Ghirlanda relation assumes the extreme value $f_B = 1$. However, we can create less rigorous yet still relevant tests by comparing the observed distributions of these ratios to calculated distributions based on model redshift and beaming fraction distributions. Applying this model dependent test, we find that the observed and model distributions are discrepant, although the discrepancy is less extreme for the Ghirlanda relation than for the Amati relation.

Similar to Nakar & Piran, we suspect that the Amati relation, and to a lesser extent the Ghirlanda relation, result from selection effects affecting the burst sample used to discover and calibrate this relation. The calibrating sample falls on the high fluence, low E_p edge of the BATSE sample. While our results show that these relations are not valid for the entire BATSE sample, they do not preclude their validity for a sub-population, although for the Amati relation this sub-population is small.

In the next section (§2) we present the methodology behind our tests. The following section (§3) describes our data. We then discuss the results (§4) and present our conclusions (§5).

2. Methodology

The Amati relation is

$$E_p = C_1 \left(\frac{E_{\rm iso}}{10^{52}\ {\rm erg}} \right)^{\eta_1} \tag{1}$$

where E_p is the peak energy for the 'fluence spectrum' (the spectrum averaged over the entire burst) in the burst frame and $E_{\rm iso}$ is the isotropic energy, the burst energy if the observed flux were emitted in all directions. Friedman & Bloom (2004) find $C_1 = 95 \pm 11$ keV and $\eta_1 = 0.5 \pm 0.04$; we use $C_1 = 95$ keV and $\eta_1 = 0.5$ for our calculations.

The Ghirlanda relation is

$$E_p = C_2 \left(\frac{E_\gamma}{10^{51}\ {\rm erg}} \right)^{\eta_2} \tag{2}$$

where E_γ is the total energy actually radiated. Friedman & Bloom find $C_2 = 512 \pm 15$ keV and $\eta_2 = 0.70 \pm 0.07$; we use $C_2 = 512$ keV and $\eta_2 = 0.7$.

The peak energy in the observer's frame is

$$E_{p,obs} = E_p/(1+z) \tag{3}$$

where z is the burst's redshift. The total energy radiated is

$$E_\gamma = E_{\rm iso}\,(1-\cos\theta_j) = f_B E_{\rm iso} \tag{4}$$

where θ_j is the jet opening angle and f_B is the beaming fraction, which is determined observationally from modelling the evolution of the afterglow. The isotropic energy is

$$E_{\rm iso} = \frac{4\pi S_\gamma d_L^2}{1+z} \tag{5}$$

where S_γ is the bolometric fluence and d_L is the luminosity distance.

Consequently, the Amati relation implies

$$\xi_1 = \frac{E_{p,obs}^2}{S_\gamma} = \frac{4\pi d_L^2 C_1^2}{[10^{52}\ {\rm erg}]\,(1+z)^3} = A_1(z) \quad . \tag{6}$$

The Ghirlanda relation implies

$$\xi_2 = \frac{E_{p,obs}^{1.429}}{S_\gamma} = f_B \frac{4\pi d_L^2 C_2^{1.429}}{[10^{51}\ {\rm erg}]\,(1+z)^{2.429}} = f_B A_2(z) \quad . \tag{7}$$

Since $f_B = (1-\cos\theta_j)$ ranges between 0 and 1, $A_2(z)$ is the upper limit to the ξ_2 ratio.

Assuming $\Omega_m = 0.3$, $\Omega_\Lambda = 0.7$, and $H_0 = 70$ Mpc/km/s, Figure 1 shows $A_1(z)$ (dashed curve) and $A_2(z)$ (solid curve), respectively. As Nakar & Piran (2005) pointed out, observed values of ξ_1 that exceed the maximum value of $A_1(z) = 1.1 \times 10^9$ cannot satisfy the Amati relation (note that Nakar & Piran scaled ξ_1 by 8×10^{-10}). Similarly, observed values of ξ_2 that exceed the maximum value of $A_2(z) = 2.9 \times 10^{10}$ cannot satisfy the Ghirlanda relation. Since $A_1(z)$ and $A_2(z)$ are both 0 at $z = 0$, both ratios do not have useful lower bounds.

These tests are rigorous but understate any inconsistency between the data and the proposed relations. $A_1(z)$ and $A_2(z)$ peak at $z = 3.8$ and $z = 12.6$, respectively, both redshifts greater than the redshifts where most bursts are thought to originate. In addition, the jet opening angle is generally small such that $f_B = (1-\cos\theta_j) \simeq \theta_j^2/2 \ll 1$. The maximum values of $A_1(z)$ and $A_2(z)$ provide absolute tests of whether observed values of ξ_1 and ξ_2 can possibly satisfy the Amati and Ghirlanda relations, respectively. However, we construct model-dependent tests that compare the observed distributions of ξ_1 and ξ_2 with distributions resulting from convolving $A_1(z)$ and $A_2(z)$ with models of the burst redshift and beaming fraction distributions.

Thus, if $p(z) \propto dN/dz$ is the redshift probability distribution then

$$P(>\xi_1)_{\rm model} = \int dz\, p(z) H\left[A_1(z) - \xi_1\right] \quad , \tag{8}$$

where $H(x)$ is the Heaviside function, 1 for $x \geq 0$ and 0 otherwise. The burst rate is assumed to follow the star formation rate, and we use $p(z)$ based on the star formation rate in Rowan-Robinson (2001); we found the same qualitative results using the star formation rates parameterized in Guetta, Piran & Waxman (2004) based on the rates of Rowan-Robinson (1999) and Porciani & Madau (1999).

Next, if $p(f_B)$ is the probability distribution for f_B then

$$P(> \xi_2)_{\rm model} = \int df_B \, p(f_B) \int dz \, p(z) H \left[f_B A_2(z) - \xi_2 \right] \quad . \tag{9}$$

Note that we assume that the beaming fraction does not evolve with redshift. As we discuss below, the results are sensitive to $p(f_B)$.

3. Data

We use a sample of 760 BATSE bursts for which we have both spectral fits to their 'fluence spectra' and energy fluences. The 16 channel CONT spectra of bursts between April 1991 and August 1996 (the 4th BATSE catalog—Paciesas et al. 1999) with sufficient fluxes were fit with a number of different spectral models (Mallozzi et al. 1998); we use the $E_{p,obs}$ from the fits with the 'Band' function (Band et al. 1993).

The fluences are from the 4th BATSE catalog (Paciesas et al. 1999). The catalog presents 20–2000 keV fluences, which we treat as bolometric. Bloom, Frail & Sari (2001) showed that the k-correction for burst spectra is of order unity, and Friedman & Bloom (2004) use a k-correction to shift the fluence's energy band to 20–2000 keV in the burst frame (which requires the burst redshift). Jimenez, Band & Piran (2001) showed that the fluences resulting from fitting high resolution spectra and from the processing pipeline used to create the BATSE catalog can differ by up to a factor of 2. This provides a measure of the uncertainty in the fluence and indicates that attempts to extend the energy band of the fluence using the spectral fits is unnecessary.

4. Results

Figure 1 shows that the maximum value of the ratio $E_{p,obs}^2/S_\gamma = 1.1 \times 10^9$ occurs at $z = 3.825$. For our BATSE burst database, 668 out of 760 bursts, or 88% of the bursts, exceed this maximum. Even if we increase this maximum value by a factor of 2 to account for the dispersion around the Amati relation and uncertainties in the determination of $E_{p,obs}$ and S_γ, 555 out of 760 bursts, or 73% of the bursts, exceed this increased maximum. By

this rigorous test most of our bursts are inconsistent with the Amati relation. On the other hand, Figure 1 also shows that the maximum value of the ratio $E_{p,obs}^{1.43}/[f_B S_\gamma] = 2.85 \times 10^{10}$ occurs at $z = 12.577$. Assuming $f_B = 1$, only 12 out of 760 bursts, or 1.6% of the bursts, violate the Ghirlanda relation. If the ratio's maximum value is doubled to account for the dispersion around the relation and uncertainties in the observations, then only 6 out of 760 bursts, or 0.8% of the bursts violate this increased maximum.

Comparisons of the model and observed distributions of the energy ratio ξ_1 for the Amati (Figure 2) relation shows that the observed distribution is shifted to larger values by an order of magnitude. This reinforces our conclusion above that our data and the Amati relation are inconsistent.

The analysis of the Ghirlanda relation requires not only the redshift distribution but also the beaming fraction distribution; as shown by Figure 3, we find that the model distribution for the ratio ξ_2 is heavily dependent on the assumed beaming fraction distribution. Very small beaming factors result in afterglows with very early breaks in the afterglow evolution, before observations have begun, while large beaming factors lead to afterglows that break late, after the afterglow is no longer observable. Consequently the currently observed distribution of beaming factors is plagued by selection effects at both its low and high ends; these selection effects are not relevant to the BATSE database but they are largely the same effects that shaped the datasets in which the two relations were discovered. Nonetheless, Figure 3 compares the observed distribution (solid curve) to the model distribution resulting from three different estimates of the beaming fraction distribution (dashed curves). The first uses the *observed* f_B distribution found by Frail et al. (2001): $p(f_B) \propto f_B^{-1.77}$ for $\log(f_B) > -2.91$ and constant for smaller f_B. The second beaming fraction distribution is based on Guetta et al. (2004), who modelled the actual θ_j distribution as a steep power law above $\theta_{j,0} = 0.12$ radians, and a much shallower power law for smaller θ_j. Transforming θ_j into f_B using the small angle approximation $f_B \simeq \theta_j^2/2$, and converting the actual distribution into the observed distribution (a burst with a beaming factor of f_B has a probability of f_B of being observed) results in $p(f_B) \propto f_B^{-2}$ for $\log(f_B) > -2.14$ and constant for smaller f_B. Note that Guetta et al. perform a more sophisticated conversion (relying on additional modelling assumptions) from the actual to observed distributions taking into account the burst luminosity function and the distance to which bursts can be detected. The differences between these two beaming faction distributions led us to fit the values of θ_j in Friedman & Bloom (2005), resulting in the third distribution on Figure 3: $p(f_B) \propto f_B^{-1.65}$ for $\log(f_B) > -2.41$ and $p(f_B) \propto f_B^{0.7}$ for smaller f_B. For comparison, the dot-dashed curves result from constant values of $f_B = 0.0275$ and $f_B = 1$. Although $f_B = 0.0275$ maximizes the Kolmogorov-Smirnoff (K-S) probability that the model and observed distributions are drawn from the same population, this probability is still only 1.11×10^{-8}.

The first three model distributions shown on Figure 3 result from beaming factor distributions with similar power law indices for large beaming fractions but break values that differ significantly. Power law distributions with indices $\mu < -1$ (where $p(f_B) \propto f_B^{\mu}$) diverge as f_B approaches 0, and the value of the normalized probability at a given value of f_B above any break or cutoff depends on the value of this break or cutoff. The magnitude of the discrepancy between the observed and model distributions of ξ_2 differ for the three estimates of the beaming fraction distribution, but in all cases there is a real discrepancy.

Perhaps the BATSE burst consist of a number of different burst populations, only one of which satisfies the Amati or Ghirlanda relations. To test this hypothesis for each relation, we progressively removed the highest ratio from the observed distribution and calculated the K-S probability that the resulting observed and model distributions are the same. Thus for the Amati relation we first calculated the K-S probability that the observed distribution of the ratio $\xi_1 = E_{p,obs}^2/S_\gamma$ (the solid curve in Figure 2) was drawn from a model distribution (the dashed curves in Figure 2). We then sorted the observed ratio distribution. Iteratively, we removed the highest ratio, and calculated the K-S probability. We performed the same procedure for the Ghirlanda ratio for the three estimates of the beaming fraction distribution.

Table 1 shows the K-S probabilities for the total burst population and the sub-population that maximizes the K-S probability; the table also shows the fraction that this sub-population constitutes. The small K-S probabilities for the full sample for each relation quantifies the discrepancies between the observed and model distributions, which are readily apparent from Figures 2 and 3. No more than $\sim 18\%$ of the burst sample is from a sub-population satisfying the Amati relation. Whether a sub-population can satisfy the Ghirlanda relation depends on the beaming factor distribution; a larger break in the beaming factor distribution increases both the size of the sub-population that may be consistent with the Ghirlanda relation and the K-S probability of this sub-population.

The redshift distribution used above assumes that BATSE detected bursts with equal efficiency at all redshifts. However, identical bursts originating at higher redshift will be fainter and their observed spectra will be softer than their low-z counterparts. Assuming there is no compensating evolution, the detection efficiency for higher redshift bursts should be smaller, and the observed redshift distribution should be shifted to smaller redshifts. Indeed, this appears to be the case for a sample of bursts observed by BATSE that were binned with respect to intensity (Mallozzi et al. 1995). There is a strong general trend toward smaller average E_p for the weaker bursts, and the interpretation is consistent with a larger average cosmological redshift. The redshift distribution assuming redshift-independent detection efficiency peaks at $z = 1.7$, which is below the redshifts where the Amati and Ghirlanda ratios peak (the ratios shown in Figure 1). Thus shifting the observed redshift

distribution to lower z can only shift the model ratio distributions (the dashed curves in Figures 2 and 3) to lower values, increasing the discrepancy between the model and observed distributions.

5. Conclusions and Summary

We test whether the Amati relation—$E_p \propto E_{\rm iso}^{1/2}$—and the Ghirlanda relation—$E_p \propto E_\gamma^{0.7}$—are consistent with a large sample of BATSE bursts for which $E_{p,obs}$ and fluences are available. Note that E_p is in the burst frame and $E_{p,obs}$ in the Earth's frame. In the most rigorous test, where the bursts may be at any redshift and have any beaming fraction for which these relations are satisfied, we find that the Amati relation cannot be satisfied by 88% of the bursts, consistent with the results of Nakar & Piran, while the Ghirlanda relation is not satisfied by only 1.6% of the bursts.

A less rigorous test results from modelling the redshift distribution for both relations and the beaming fraction f_B distributions for the Ghirlanda relation. The model distributions of the ratios $E_{p,obs}^2/S_\gamma$ for the Amati relation and $E_{p,obs}^{1.43}/S_\gamma$ for the Ghirlanda relation are shifted to smaller values of these ratios relative to the observed distribution. The magnitude of the discrepancy for the Ghirlanda relation depends on the model for the beaming factor distribution, specifically on breaks or cutoffs in the assumed power law model at small values of f_B. We use three different model distributions based on the small number of f_B values, although we note that the set of bursts with f_B is the same set used to discover and calibrate the two relations, and thus are affected by the same selection effects, which are not relevant to the BATSE bursts.

Including a detection efficiency that decreases as the redshift increases exacerbates this discrepancy (unless there is compensating burst evolution). If we assume that the Amati or Ghirlanda relations apply to a sub-population of the entire dataset, then only $\sim 18\%$ of the BATSE burst sample can be members of this sub-population for the Amati relation, whereas the sub-population's size depends on the beaming factor distributions for the Ghirlanda relation.

These results suggest that these two relations may be artifacts of selection effects in the burst sample in which these relations were discovered. The selection effects may favor a burst sub-population for which the Amati or Ghirlanda relation is valid. Bursts for which redshifts and beaming fractions have been determined must be relatively bright and soft (low $E_{p,obs}$, the energy range in which the localizing instruments operate) to be localized and for their afterglows to be tracked. Figure 4 shows the distribution of our BATSE burst sample

in the $E_{p,obs}$–fluence plane and the bursts from the Friedman & Bloom (2004) sample; also seen are the limits resulting from the Amati (solid curve) and Ghirlanda (assuming $f_B = 1$; dashed curve) relations. We converted the fluences of the Friedman & Bloom (2004) sample to the 20 to 2000 keV band using the spectral fits in their paper; where they do not report spectral indices we used low and high energy spectral indices of $\alpha = -0.8$ and $\beta = -2.3$, respectively (Preece et al. 2000). Note that although the BATSE and Friedman & Bloom fluences are chosen to be bolometric, in reality they integrate the spectrum between different energy limits, and they result from different types of processing. As can be seen, the bursts used to calibrate these two relations (i.e., the Friedman & Bloom sample) are on the edge of the BATSE distribution, consistent with the Amati relation. As Nakar & Piran (2004) concluded, the sample of bursts with redshifts and afterglow observations have a much higher selection threshold than the BATSE distribution.

The much larger sample of bursts with redshifts, fluences and beaming fractions that Swift will collect will test these relations conclusively, may distinguish between different burst populations and may reveal truly universal relations among burst properties.

We thank Ehud Nakar and Tsvi Piran for their careful reading of our text and their insightful comments.

REFERENCES

Amati, L., et al. 2002, A&A, 390, 81

Band, D. 2001, ApJ, 563, 582

Band, D., et al. 1993, ApJ, 413, 281

Bloom, J. S., Frail, D. A., & Sari, R. 2001, AJ, 121, 2879

Frail, D. A., et al. 2001, ApJ, 562, L55

Friedman, A. S. & Bloom, J. S. 2004, ApJ, submitted [astro-ph/0408413]

Guetta, D., Piran, T., & Waxman, E. 2004 ApJ, in press [astro-ph/0311488]

Jimenez, R., Band, D. & Piran, T. 2001, ApJ, 561, 171

Mallozzi, R. S., Paciesas, W. S., Pendleton, G. N., Briggs, M. S., Preece, R. D., Meegan, C. A., & Fishman, G. J. 1995, ApJ, 454, 597

Mallozzi, R., et al. 1998, in Gamma-Ray Bursts, 4th Huntsville Symposium, AIP Conference Proceedings 428, eds. C. Meegan, R. Preece and T. Koshut (AIP: Woodbury, NY), 273

Paciesas, W., et al. 1999, ApJS, 122, 465

Preece, R. D., Briggs, M. S., Mallozzi, R. S., Pendleton, G. N., Paciesas, W. S., & Band, D. L. 2000, ApJS, 126, 19

Porciani, C., & Madau, P., 2001, ApJ, 548, 522

Rowan-Robinson, M. 1999, Ap&SS, 266, 291

Rowan-Robinson, M. 2001, ApJ, 549, 745

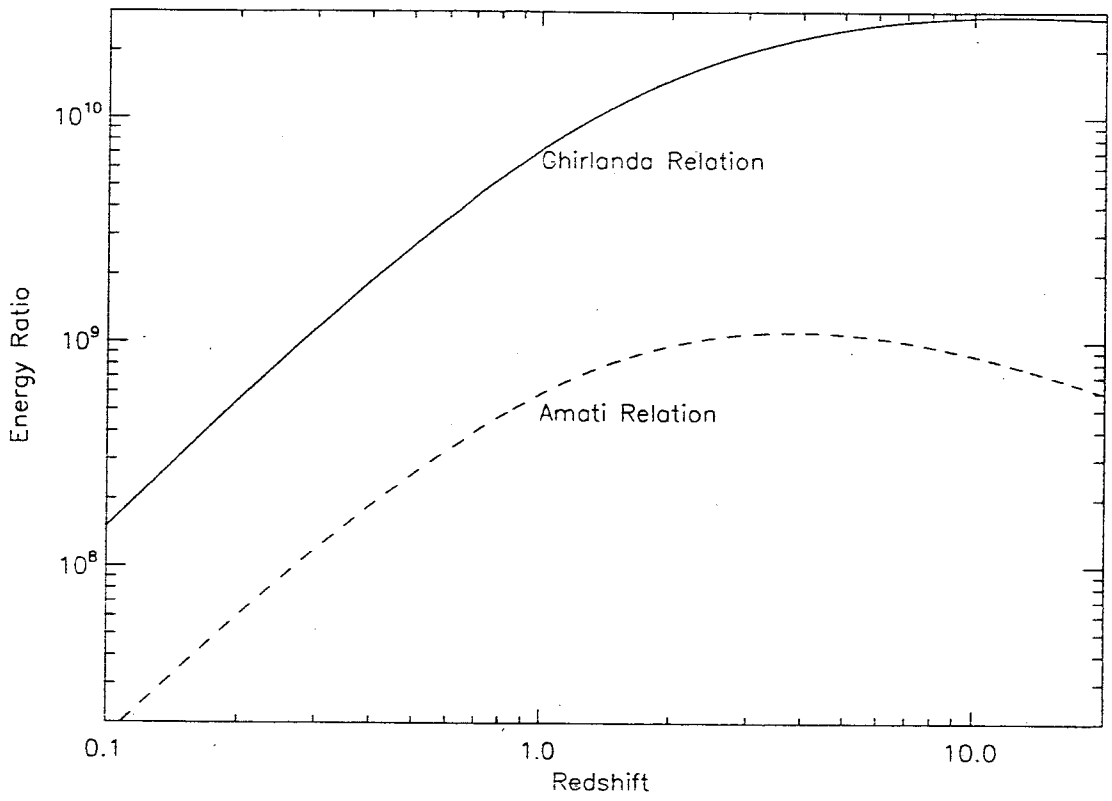

Fig. 1.— Value of the Amati relation energy ratio $E^2_{p,obs}/S_\gamma$ (dashed curve) and Ghirlanda relation energy ratio $E^{1.43}_{p,obs}/[f_B S_\gamma]$ (solid curve) as a function of redshift.

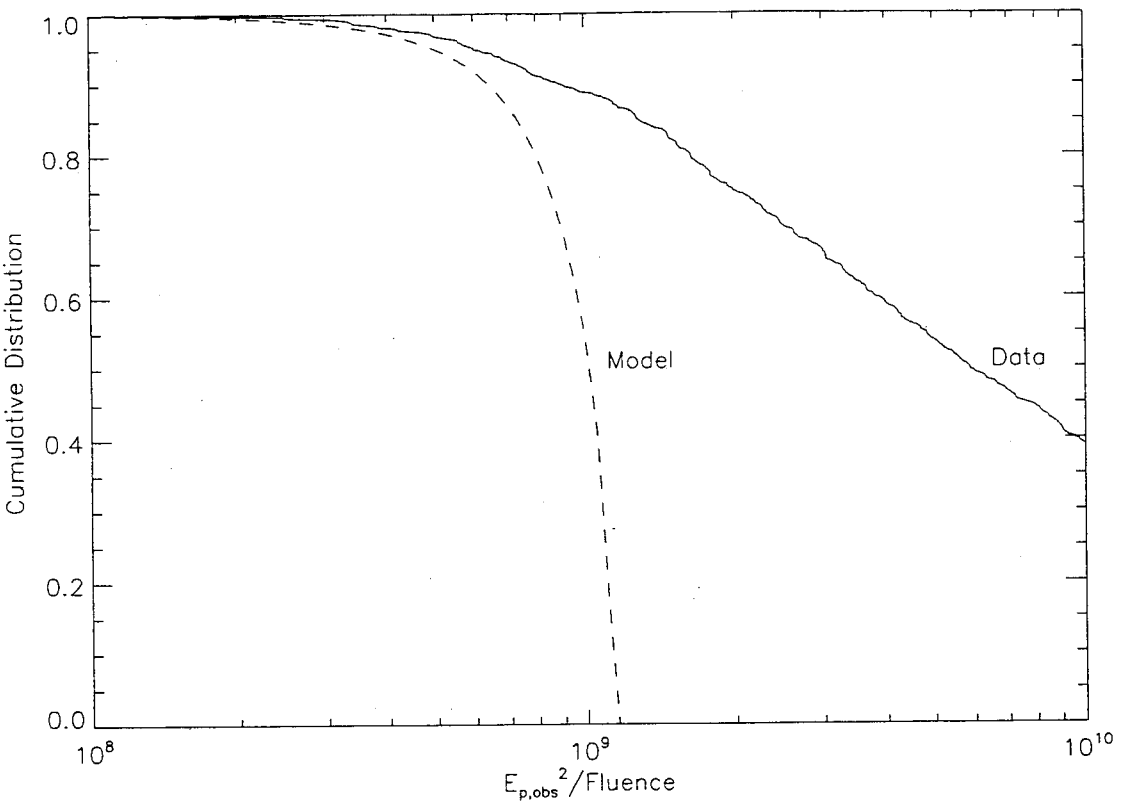

Fig. 2.— Observed (solid curve) and model (dashed curve) distributions of the ratio $E^2_{p,obs}/S_\gamma$. If the Amati relation and the assumed redshift distribution are both valid then these ratio distributions should be the same.

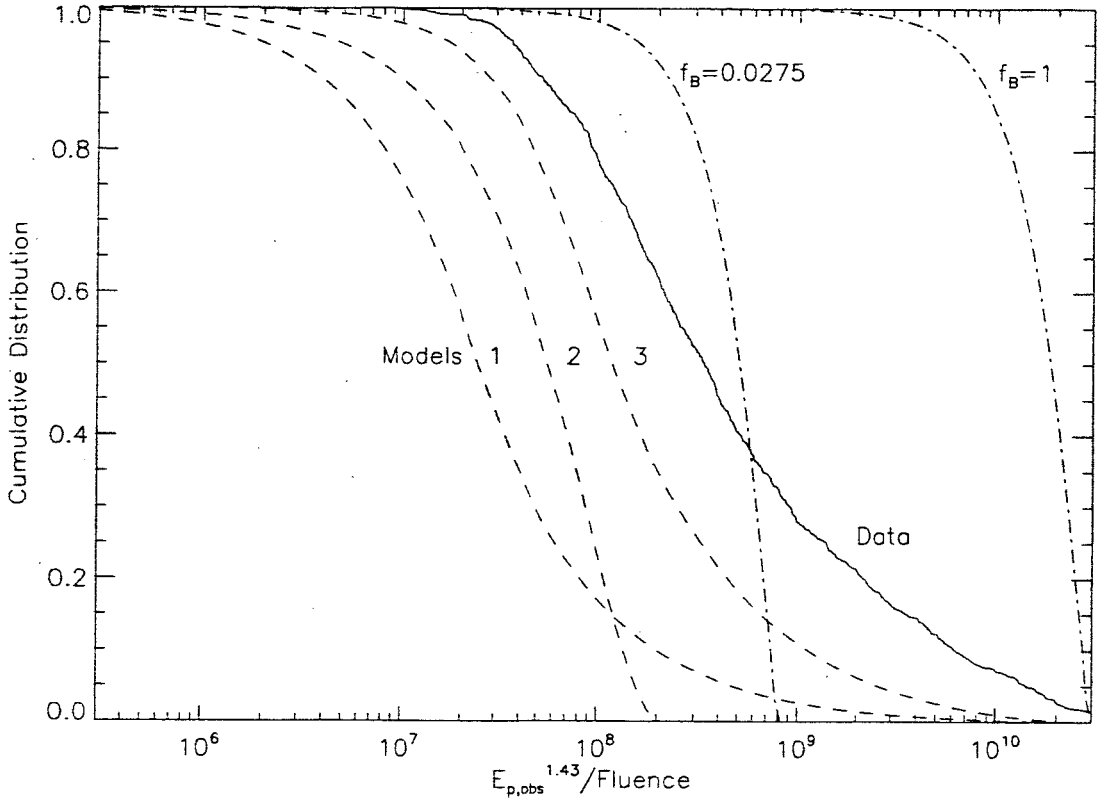

Fig. 3.— Observed (solid curve) and model (dashed curves) distributions of the Ghirlanda relation's energy ratio $E_{p,obs}^{1.43}/[f_B S_\gamma]$. The dashed curves result from the beaming fraction distributions of Frail et al. (2001; labelled 1), Guetta et al. (2004; labelled 2) and our fit (labelled 3). If the Ghirlanda relation and the assumed redshift and beaming fraction distributions are all valid then the model and observed ratio distributions should be the same. For comparison, the two dot-dashed curves shows the ratio distribution if $f_B = 0.0275$ (left) or $f_B = 1$ (right).

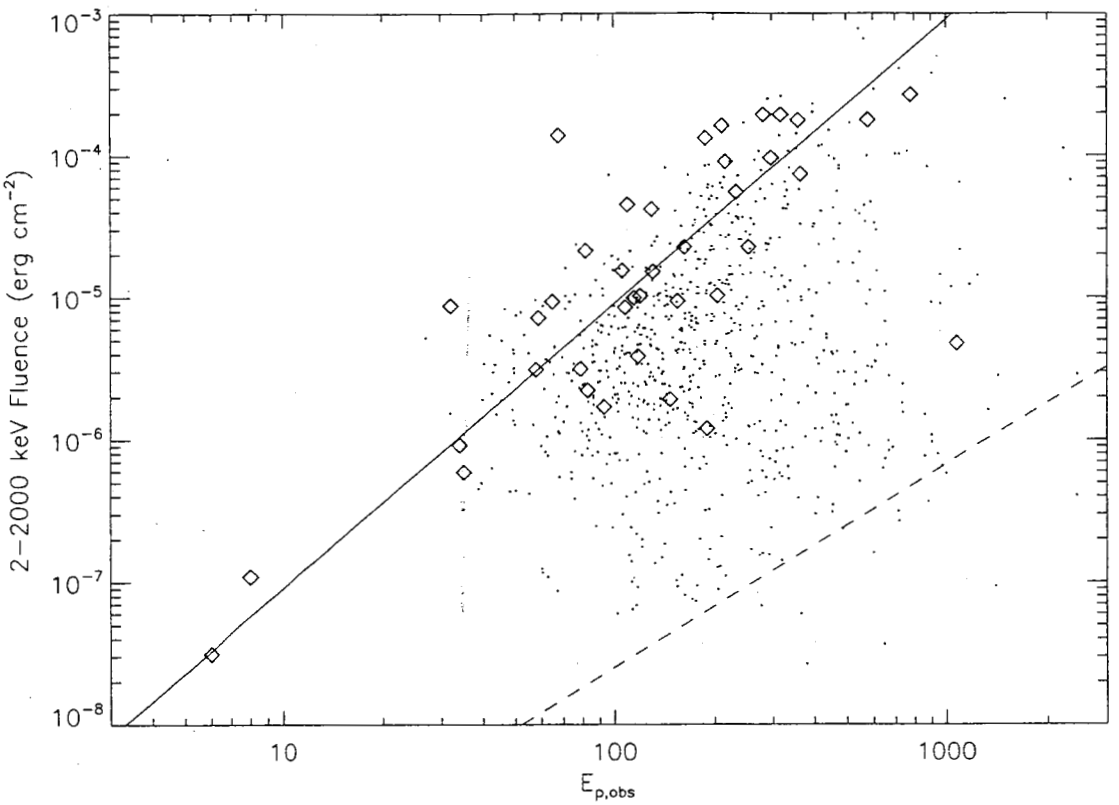

Fig. 4.— Location of bursts in the BATSE (dots) and Friedman & Bloom (2004—diamonds) samples on the $E_{p,obs}$–fluence plane. Also shown are the limits of the Amati (solid line) and Ghirlanda (for $f_B = 1$; dashed line) relations; these relations permit bursts to fall above these lines.

Table 1. Consistency Between Observed and Model Ratio Distributions

Relation	Beaming Fraction Distribution[a]	K-S Probability, Entire Population	K-S Probability, Subpopulation[b]	Subpopulation Fraction[c]
Amati	NA[d]	$< 10^{-38}$	1.1×10^{-4}	0.182
Ghirlanda	Frail et al. (2001)	5.09×10^{-33}	NA[e]	0 [e]
Ghirlanda	Guetta et al. (2004)	2.69×10^{-8}	0.236	0.614
Ghirlanda	This paper	1.56×10^{-6}	0.0761	0.658

[a]Estimate of the beaming fraction distribution.

[b]K-S probability for the sub-population that maximizes this probability.

[c]Fraction of the 760 BATSE bursts in the sub-population that maximizes the K-S probability.

[d]The beaming fraction is not required for the Amati relation.

[e]No sub-population satisfies the Ghirlanda relation for this beaming fraction model.